Supporting Information for **Efficient Separation of 1,5-dimethyl-2-pyrrolidone from N-methylpyrrolidone Enabled by Pore Confinement**

Rongkai Cui [a #], *Minlei Yin* [a, d #], *Xiaoyan Chen* [c], *Xiaoyu Lou* [a], *Chen Yang* [a], *Ting Qiu* [a, b, *] ，*Jie Chen* [a, *]

[a] *State Key Laboratory of Green and Efficient Development of Phosphorus Resources, Engineering Research Center of Reactive Distillation, Fujian Province University, College of Chemical Engineering, Fuzhou University, Fuzhou 350108, Fujian;*

[b] *Qingyuan Innovation Laboratory, Quanzhou, Fujian*

[c] *Fuzhou University International Joint Laboratory of Thermochemical Conversion of Biomass, Fuzhou University, Fuzhou 350108, Fujian;*

[d] *School of Chemical Engineering and Dyeing Engineering, Henan University of Engineering, Zhengzhou 450007, Henan*

[#] *These authors contributed equally.*

*** Corresponding authors:**

Prof. Jie Chen, Tel: +8618750716952; Email: jiechen@fzu.edu.cn;

Prof. Ting Qiu, Tel: +8618960870909; Email: tingqiu@fzu.edu.cn.

Table S1 Specific surface area and pore analysis of α-CD-230, β-CD-230, and γ-CD-230

Sample	S_{BET} (m^2 g^{-1})	V_{total} (cm^3 g^{-1})	V_{mic} (cm^3 g^{-1})	V_{meso} (cm^3 g^{-1})	V_{mac} (cm^3 g^{-1})
α-CD-230	7	0.09	0	0.03	0.06
β-CD-230	0	0.09	0	0.09	0
γ-CD-230	2	0	0	0	0

Table S2 Elemental analysis of α-CD-230, β-CD-230, and γ-CD-230

Sample	C (wt%)	H (wt%)	O (wt%)	H/O (wt%)
α-CD	44.37	6.20	49.53	12.52
β-CD	44.49	6.20	49.31	12.57
γ-CD	44.38	6.23	49.39	12.61
α-CD-230	70.42	4.55	25.03	18.18
β-CD-230	71.10	4.63	24.19	19.14
γ-CD-230	70.63	4.55	24.62	18.48

Table S3 Specific surface area and pore analysis of α-CD-800, β-CD-800, and γ-CD-800

Sample	S_{BET} (m^2 g^{-1})	V_{total} (cm^3 g^{-1})	V_{mic} (cm^3 g^{-1})	V_{meso} (cm^3 g^{-1})	V_{mac} (cm^3 g^{-1})
α-CD-800	389	0.25	0.14	0.04	0.07
β-CD-800	392	0.26	0.15	0.03	0.08
γ-CD-800	362	0.25	0.14	0.03	0.08

Table S4 Elemental analysis of α-CD-800, β-CD-800, and γ-CD-800

Sample	C (wt%)	H (wt%)	O (wt%)	H/C (%)	O/C (%)
α-CD-800	89.320	2.014	5.435	2.255	6.085
β-CD-800	93.100	1.110	5.930	1.192	6.369
γ-CD-800	89.960	1.870	5.224	2.079	5.807

Table S5 Specific surface area and pore analysis of β-CD-500, β-CD-600, β-CD-700, β-CD-800, and β-CD-900

Sample	S_{BET} ($m^2\ g^{-1}$)	V_{total} ($cm^3\ g^{-1}$)	V_{mic} ($cm^3\ g^{-1}$)	V_{meso} ($cm^3\ g^{-1}$)	V_{mac} ($cm^3\ g^{-1}$)
β-CD-500	0	0.08	0	0.08	0
β-CD-600	350	0.22	0.13	0.02	0.07
β-CD-700	383	0.22	0.11	0.03	0.08
β-CD-800	392	0.26	0.15	0.03	0.08
β-CD-900	517	0.22	0.21	0.02	0

Table S6 Elemental analysis of β-CD-500, β-CD-600, β-CD-700, β-CD-800, and β-CD-900

Sample	C (wt%)	H (wt%)	O (wt%)	H/C (%)	O/C (%)
β-CD-500	85.84	3.31	10.59	3.86	12.34
β-CD-600	90.15	2.55	7.80	2.83	8.65
β-CD-700	92.48	1.65	6.63	1.78	7.17
β-CD-800	93.10	1.11	5.93	1.19	6.37
β-CD-900	93.29	1.03	5.03	1.10	5.39

Table S7 Specific surface area and pore analysis of α-600, α-700, and α-800

Sample	S_{BET} (m^2 g^{-1})	V_{total} (cm^3 g^{-1})	V_{mic} (cm^3 g^{-1})	V_{meso} (cm^3 g^{-1})	V_{mac} (cm^3 g^{-1})
α-600	3	0.10	0	0.09	0.01
α-700	313	0.26	0.12	0.03	0.09
α-800	418	0.27	0.16	0.03	0.08

Table S8 Specific surface area and pore analysis of β-600, β-700, and β-800

Sample	S_{BET} (m^2 g^{-1})	V_{total} (cm^3 g^{-1})	V_{mic} (cm^3 g^{-1})	V_{meso} (cm^3 g^{-1})	V_{mac} (cm^3 g^{-1})
β-600	49	0.11	0.02	0.02	0.07
β-700	338	0.23	0.13	0.03	0.07
β-800	379	0.25	0.15	0.02	0.08

Table S9 Specific surface area and pore analysis of γ-600, and γ-700

Sample	S_{BET} (m^2 g^{-1})	V_{total} (cm^3 g^{-1})	V_{mic} (cm^3 g^{-1})	V_{meso} (cm^3 g^{-1})	V_{mac} (cm^3 g^{-1})
γ-700	288	0.20	0.11	0.01	0.08
γ-800	366	0.26	0.14	0.04	0.08

Table S10 Elemental analysis of β-600, γ-600, α-700, α-800, and β-800

Sample	C (wt%)	H (wt%)	O (wt%)	H/C (%)	O/C (%)
β-600	91.23	2.09	3.12	2.29	3.42
γ-700	92.19	2.06	2.98	2.23	3.23
α-700	94.72	1.28	3.24	1.35	3.42
α-800	94.63	0.69	0.78	0.73	0.82
β-800	95.39	0.79	0.99	0.82	1.04

Table S11 Adsorption isotherm parameters of β-CD-600, β-CD-700, and β-CD-800 at 25 °C

Temperature (°C)	Sample	Langmuir			Freundlich		
		Q_m (mg g^{-1})	K_L (kg g^{-1})	R^2	K_F (mg g^{-1})	n	R^2
25	β-CD-600	61.7	1.5×10^{-3}	0.998	1.99	2.39	0.981
	β-CD-700	160.3	1.3×10^{-3}	0.992	3.90	2.22	0.973
	β-CD-800	142.7	1.4×10^{-3}	0.991	3.49	2.20	0.972

Table S12 Adsorption isotherm parameters of α-700, γ-600, α-800, and β-800 at 25 °C

	Sample	Langmuir			Freundlich		
		Q_m (mg g^{-1})	K_L (kg g^{-1})	R^2	K_F (mg g^{-1})	n	R^2
Temperature （°C）	α-700	73.9	1.7×10^{-3}	0.997	2.36	2.36	0.964
	γ-700	45.3	1.3×10^{-3}	0.990	1.18	1.18	0.952
	α-800	168.1	2.0×10^{-3}	0.997	7.33	7.33	0.955
	β-800	202.8	1.7×10^{-3}	0.996	7.72	7.72	0.976

Table S13 Kinetic fitting parameters of β-800 for DMP adsorption at different initial concentrations

Concentration (mg kg^{-1})	Pseudo-first-order model			Pseudo-second-order model		
	Q_e (mg g^{-1})	k_1 (kg g^{-1})	R^2	Q_e (mg g^{-1})	k_2 (g mg^{-1} min^{-1})	R^2
296	37.4	1.89×10^{-2}	0.962	48.3	6.69×10^{-4}	0.997
450	122	3.43×10^{-2}	0.896	78.7	2.57×10^{-3}	0.997

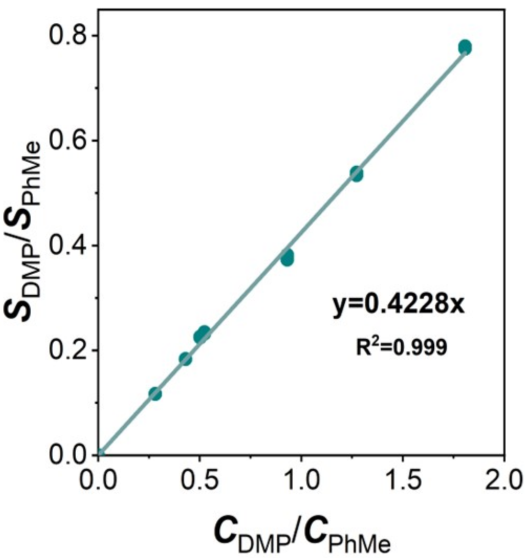

Fig. S1 Standard curve for DMP quantification.

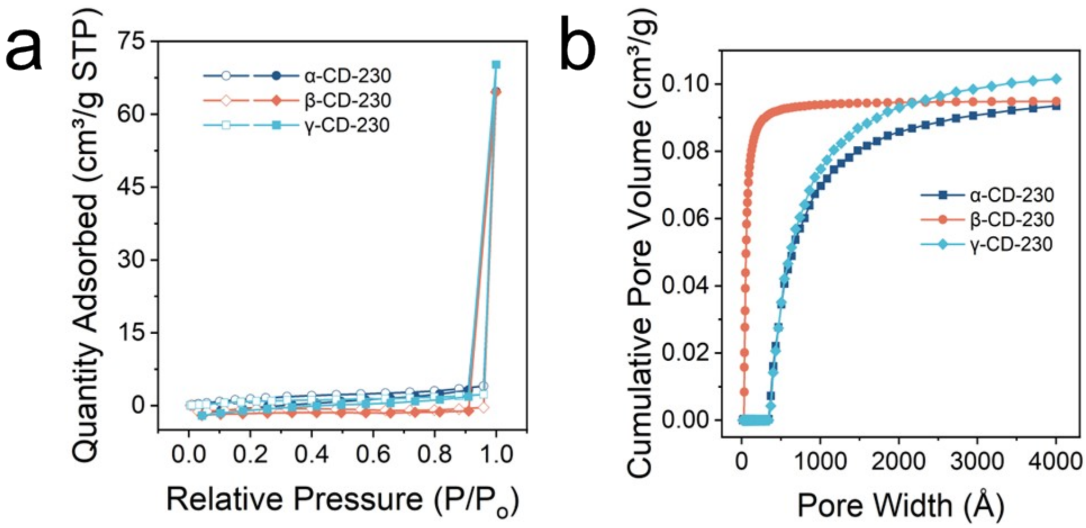

Fig. S2 (a) N_2 sorption isotherm, and (b) cumulative pore volume distribution of α-CD-230, β-CD-230 and γ-CD-230.

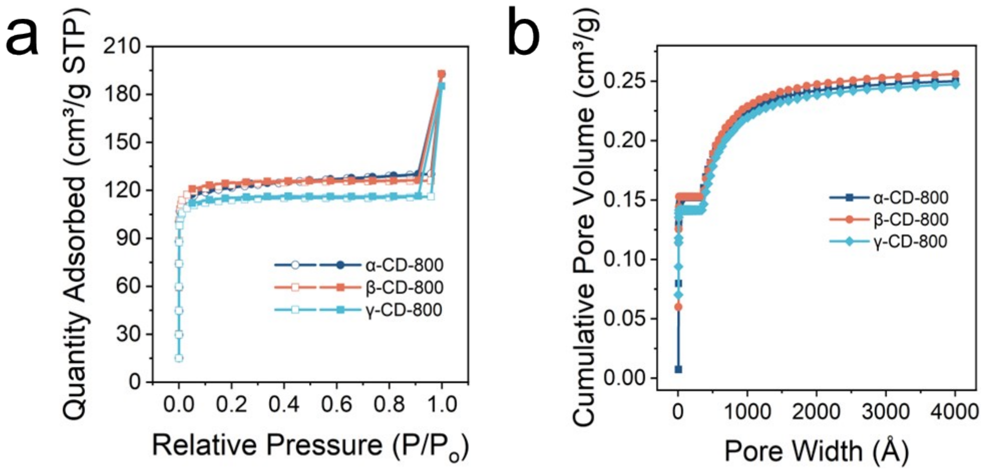

Fig. S3 (a) N_2 sorption isotherm, and (b) cumulative pore volume distribution of α-CD-800, β-CD-800, and γ-CD-800.

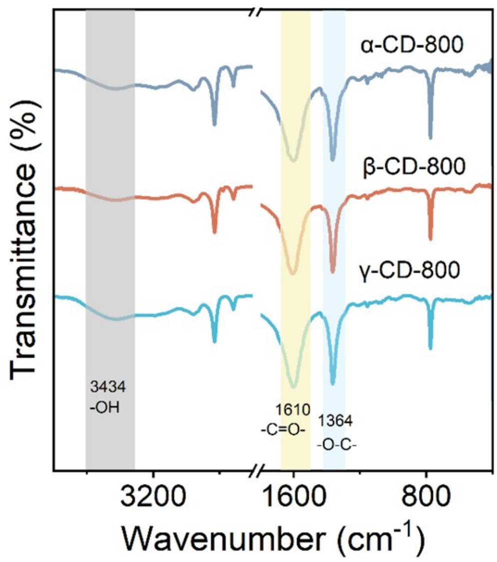

Fig. S4 FT-IR spectra of α-CD-800, β-CD-800, and γ-CD-800.

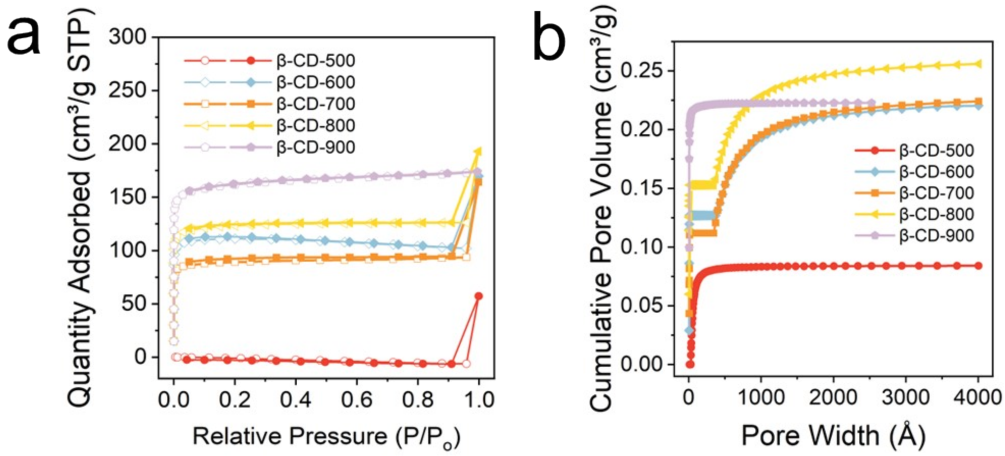

Fig. S5 N_2 sorption isotherm, and (b) cumulative pore volume distribution of β-CD-500, β-CD-600, β-CD-700, β-CD-800, and β-CD-900.

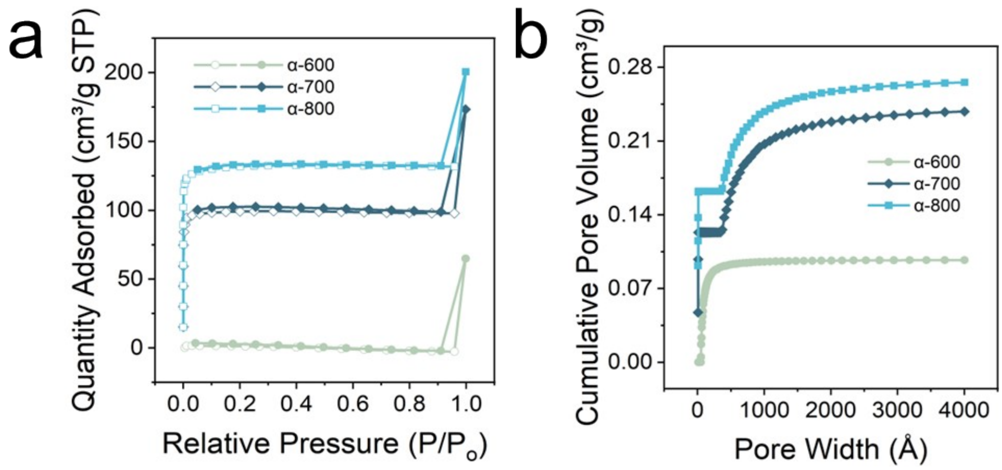

Fig. S6 N_2 sorption isotherm, and (b) cumulative pore volume distribution of α-600, α-700, and α-800.

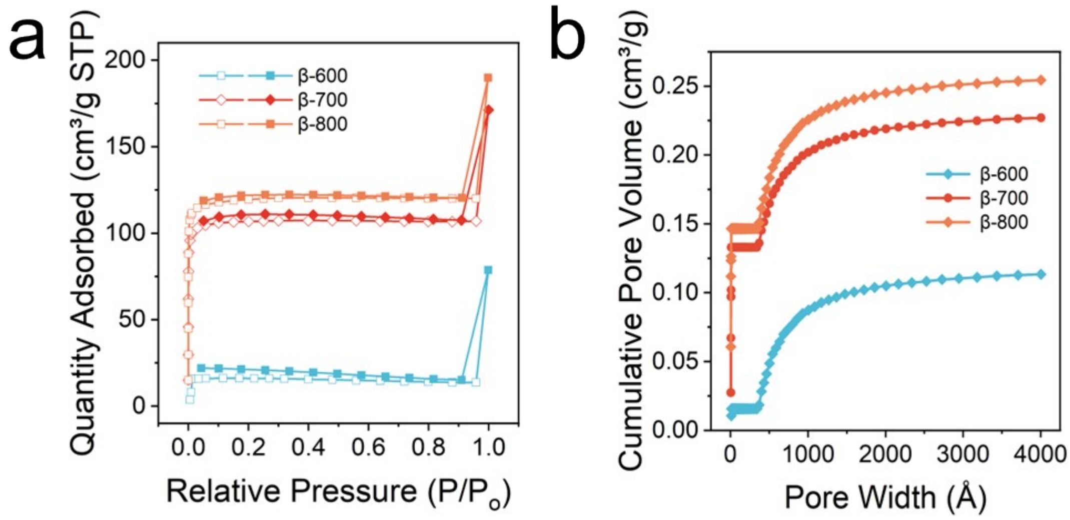

Fig. S7 N_2 sorption isotherm, and (b) cumulative pore volume distribution of β-600, β-700, and β-800.

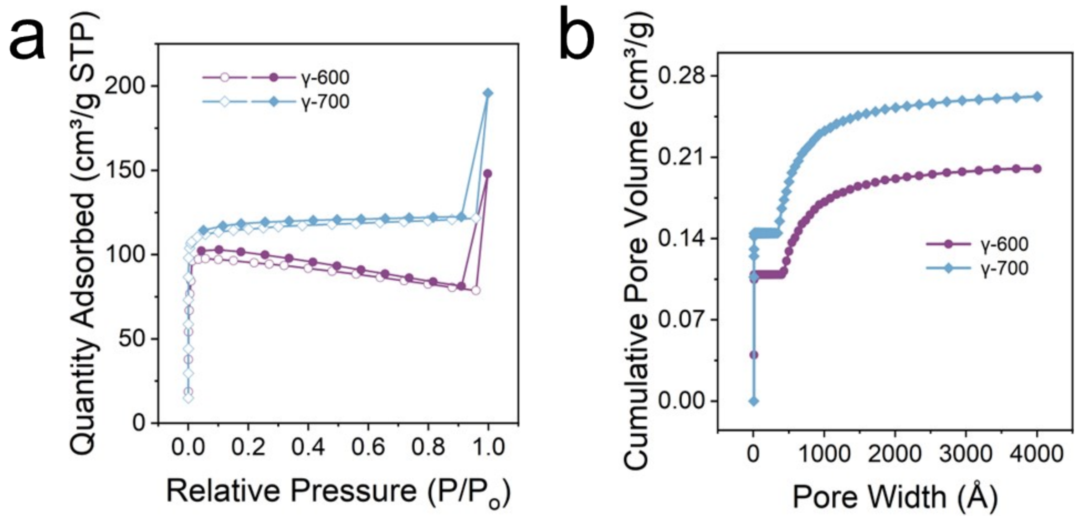

Fig. S8 N_2 sorption isotherm, and (b) cumulative pore volume distribution of γ-600, and γ-700.

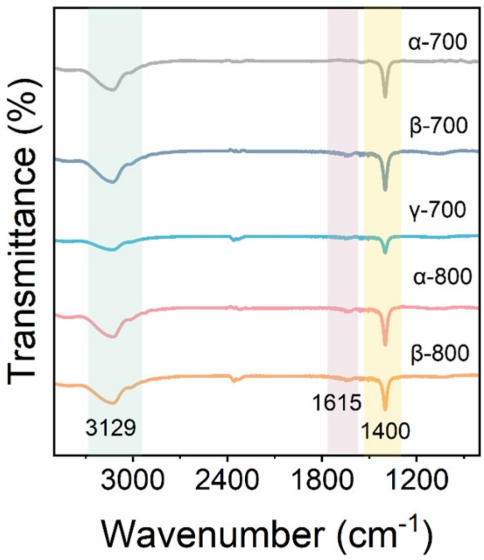

Fig. S9 FT-IR spectra of α-800, α-700, γ-700, β-700 and β-800.

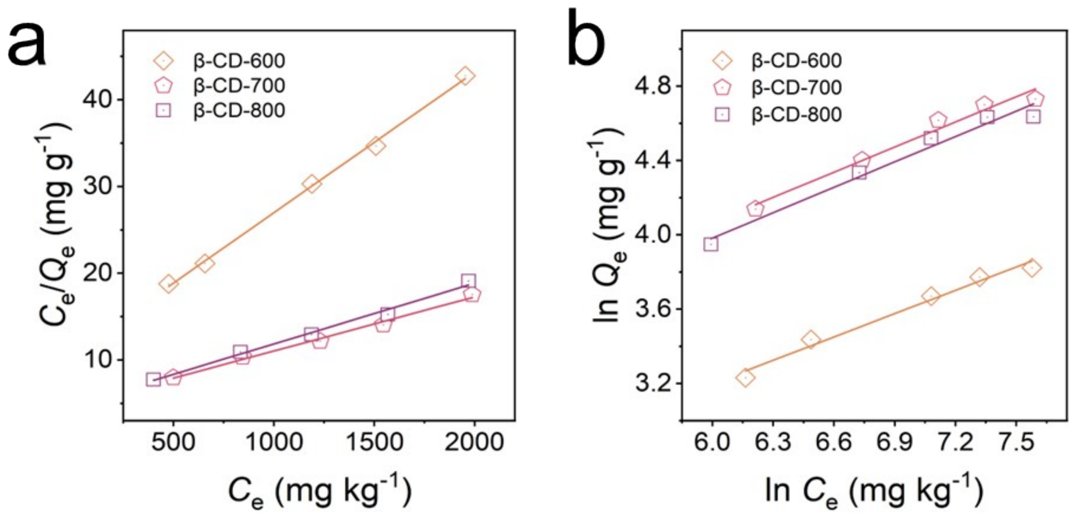

Fig. S10 Isothermal adsorption data for DMP onto β-CD-600, β-CD-700, and β-CD-800 were fitted to (a) the Langmuir model and (b) the Freundlich model.

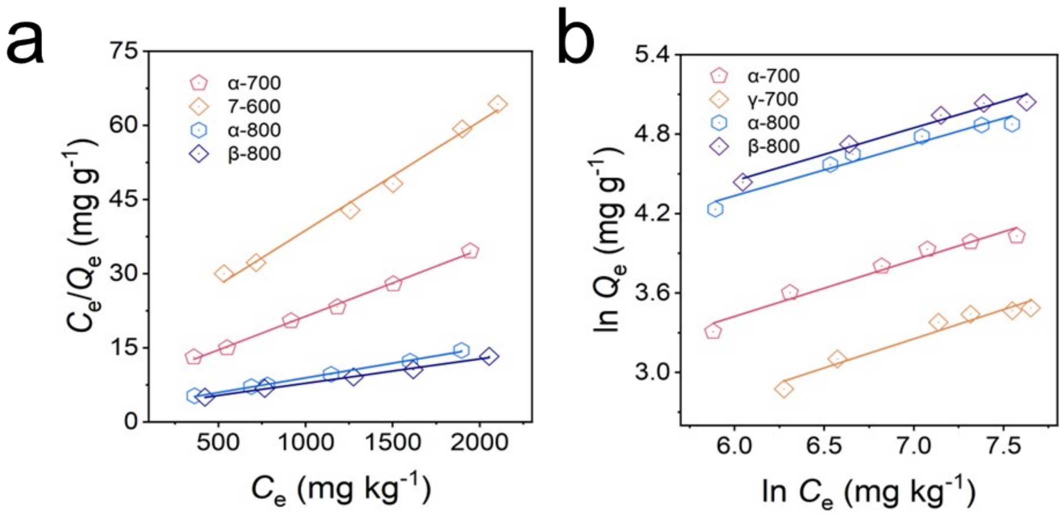

Fig. S11 Isothermal adsorption data for DMP onto α-700, γ-700, α-800, and β-800 were fitted to (a) the Langmuir model and (b) the Freundlich model.

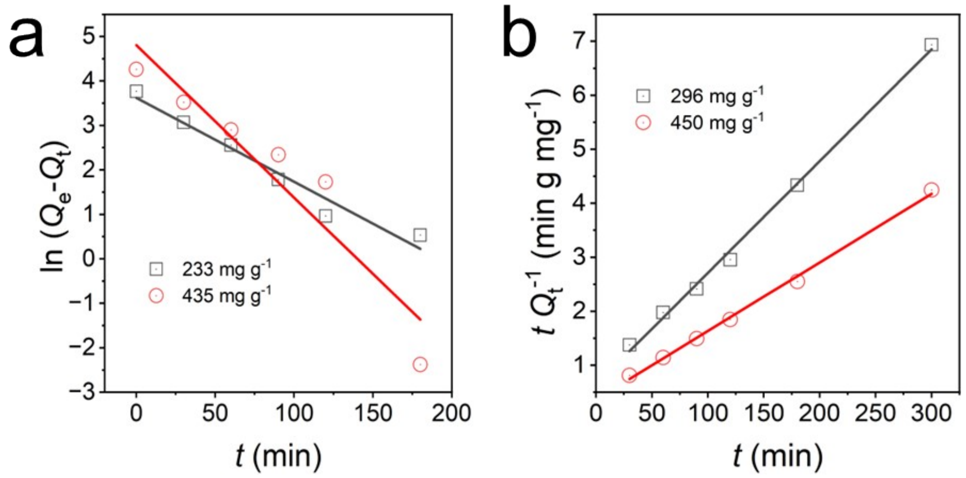

Fig. S12 Adsorption kinetic data of DMP onto β-800 at different concentrations fitted using (a) the pseudo-first-order model, and (b) the pseudo-second-order model.

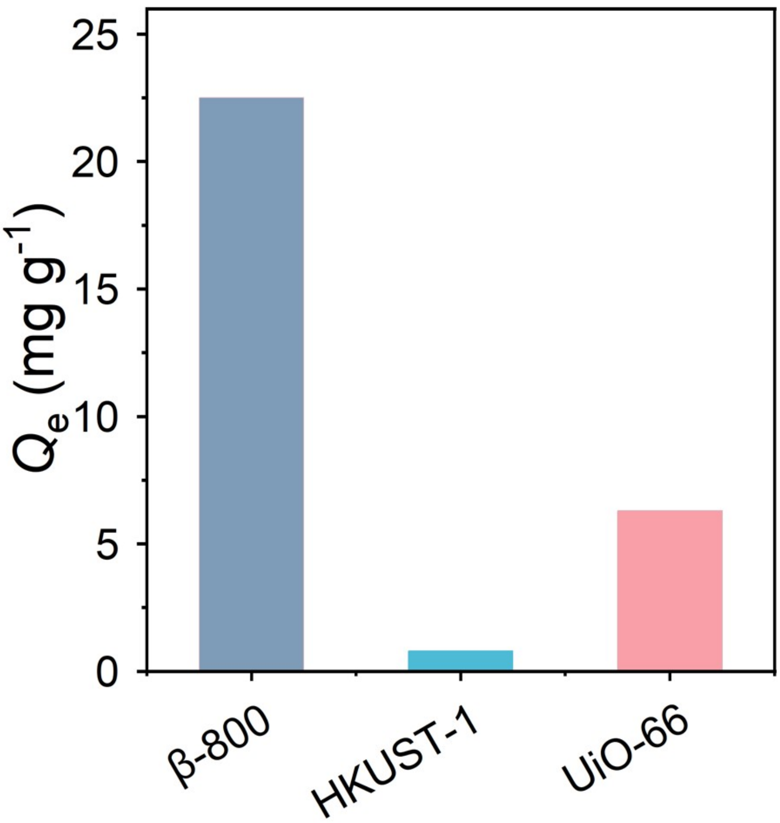

Fig. S13 Comparison of adsorption capacity of β-800, HKUST-1, and UiO-66 for DMP at an initial concentration of 416 mg kg^{-1}.